Electronic Supplementary Material (ESI) for Journal of Materials Chemistry A.

Electronic Supplementary Information (ESI) for

Phosphoric acid and post-thermal treatments reveal the peculiar role of surface oxygen anions in lithium and manganese-rich layered oxides

Jiarong He[1,†], *Weibo Hua*[1,2,†,*], *Aleksandr Missiul*[3], *Georgian Melinte*[4,5], *Chittaranjan Das*[1], *Akhil Tayal*[6], *Thomas Bergfeldt*[1], *Stefan Mangold*[7], *Xinyang Liu*[1], *Joachim R. Binder*[1], *Michael Knapp*[1], *Helmut Ehrenberg*[1], *Sylvio Indris*[1,*], *Björn Schwarz*[1], *Julia Maibach*[1,*]

[1] Institute for Applied Materials (IAM), Karlsruhe Institute of Technology (KIT), Hermann-von-Helmholtz-Platz 1, 76344 Eggenstein-Leopoldshafen, Germany.

E-mail: julia.maibach@kit.edu; sylvio.indris@kit.edu (lead contact).

[2] State Key Laboratory of Electronic Thin Films and Integrated Devices, University of Electronic Science and Technology of China, Chengdu, 610054 China.

E-mail: weibo.hua@uestc.edu.cn.

[3] CELLS-ALBA Synchrotron, Cerdanyola del Valles, E-08290 Barcelona, Spain.

[4] Institute of Nanotechnology, Karlsruhe Institute of Technology (KIT), Hermann-von-Helmholtz-Platz 1, D-76344, Eggenstein-Leopoldshafen, Germany.

[5] Helmholtz Institute Ulm (HIU) Electrochemical Energy Storage, Helmholtz Strasse 11, 89081 Ulm, Germany.

[6] Deutsches Elektronen-Synchrotron DESY, Notkestrasse 85, D-22607 Hamburg, Germany.

[7] Institute for Photon Science and Synchrotron Radiation, Karlsruhe Institute of Technology (KIT), Hermann-von-Helmholtz-Platz1, D-76344 Eggenstein-Leopoldshafen, Germany.

[†] These authors contributed equally to this work.

S1 Experimental

S1.1 Materials synthesis

Synthesis of layered LLNMO material

The Mn-rich $Li_{1.2}Ni_{0.2}Mn_{0.6}O_2$ (LLNMO) oxide was synthesized through a hydroxide co-precipitation method and a high temperature lithiation process as below.

$$0.2Ni^{2+}+0.6Mn^{2+}+2OH^{-}\xrightarrow[NH_3\cdot H_2O]{NaOH}\xrightarrow[12\text{ h}]{100°C}\text{LLNMO Precusor}$$

$$\text{LLNMO Precusor}+1.2LiOH\xrightarrow[6\text{ h}]{550°C,\text{ Air}}\xrightarrow[12\text{ h}]{850°C,\text{ Air}}Li_{1.2}Ni_{0.2}Mn_{0.6}O_2$$

A stoichiometrically mixed aqueous $NiSO_4\cdot 6H_2O/MnSO_4\cdot H_2O$ solution (Ni: Mn molar ratio=1: 3) was pumped into a continuously stirred reactor with a feeding rate of 2 ml min^{-1}. Simultaneously, 4 M NaOH solution (precipitant agent) and the desired amount of $NH_3\cdot H_2O$ (complexing agent) were fed into the reactor. The pH value, temperature, and stirring speed were precisely controlled to 11.3 ± 0.3, 52 ± 2 °C and 500 rpm, respectively. The whole synthesis process was conducted in N_2 atmosphere. After the co-precipitation, the precipitates were collected, filtered and washed with deionized water (DI-water) for several times to remove Na^+ and SO_4^{2-} ions and finally dried at 100 °C for 12 h.

The obtained LLNMO precursor was thoroughly mixed with 7 % excess of LiOH by a dry-grind and a wet-milling process with ethanol. After that, the mixture was preheated at 550 °C for 6 h and subsequently calcined at 850 °C for 12 hours in a conventional furnace under air atmosphere to obtain the layered LLNMO material.

For comparison, the spinel $LiNi_{0.5}Mn_{1.5}O_4$ cathode material was also prepared in the same synthesis procedure as a reference for Raman measurement, in which the molar ratio of transitional metal (Ni&Mn) and lithium in the mixture is 1: 0.570.

Chemical treatment of layered LLNMO material

The 4% and 5% phosphoric acid solutions (mass concentration) were prepared with DI-Water and homogenously stirred for 12 h (1000 rpm) at room temperature. Then 500 mg LLNMO particles were immersed into 4% and 5% phosphoric acid solution (2500 mg). After that, the LLNMO suspension was continuously stirred at room temperature for 2 h (1000 rpm). The LLNMO particles were collected by centrifugation, washed several times with DI-water and ethanol and finally dried at 80 °C for 12 h.

S1.2 Materials characterization

***Ex situ* synchrotron radiation diffraction (SRD).**

The phase composition and the crystal structure of ex-situ samples were measured at the high-resolution P02.1 powder diffraction beamline, storage ring PETRA-III at Deutsches Elektronensynchrotron (DESY) in Hamburg, Germany. The measurements were performed with synchrotron radiation with an energy of 60 keV and a sample exposure time of 60 s. The diffraction patterns at the P02.1 beamline were collected using a two-dimensional (2D) flat panel detector (Perkin-Elmer amorphous Silicon detector) with a sample-to-detector distance of 1600 mm. The resulting 2D images were integrated to one-dimensional diffraction patterns using a X-ray image processing program (Fit2D). The lattice structure parameters and phase fractions were refined using the Rietveld method in the program FullProf.

High-Temperature synchrotron radiation diffraction (HTSRD).

The high-temperature SRD experiments were measured at the high-resolution Materials Science and Powder Diffraction (MSPD) beamline at ALBA (Spain). The SRD patterns were collected using a MYTHEN 1D Position Sensitive Detector with a synchrotron radiation energy of 30 keV and an exposure time of 60 s. The quartz capillary with the sample was heated using FMB Oxford hot air blower from room temperature to 900 °C and cooled back down to room temperature.

X-ray absorption spectroscopy (XAS).

The XAS measurements of ex-situ samples and in-situ coin-cells (CR2025) were performed at the P64 beamline, storage ring PETRA-III at Deutsches Elektronensynchrotron (DESY) in Hamburg, Germany. The XAS data were collected at the Mn K-edge (6539 eV) and Ni K-edge (8333 eV) in transmission mode, respectively. The reference spectra for energy correction were also simultaneously collected by measuring the corresponding transition-metal foil (Ni, Mn). The X-ray absorption near edge spectra (XANES) of the XAS spectrum were achieved by subtracting the pre-edge background from the whole absorption and normalizing to the spline fit using the ATHENA software package.

Raman. Samples were placed in a chamber under the microscope interfaced to a confocal Raman microspectrometer LabRam (Horiba Scientific, Lille, France). A video image of the sample was utilized for accurate positioning of the laser spot on the material. The excitation wavelength was 633 nm. The Raman spectra were analysed using the Labspec 6.0 software.

SEM-EDX. The morphologies of the samples were obtained with a scanning electron microscope (SEM, Zeiss Merlin) with an acceleration voltage of 10 keV. The coupled energy-dispersive X-ray analysis (EDX) was measured at a Quantax 400 system (Bruker).

TG/DSC. Thermogravimetric and differential scanning calorimetric (TG/DSC) measurements were conducted using a STA 449C Netzsch thermal analyzer with a heating rate of 10 K min^{-1} up to 900 °C and a cooling rate of 10 K min^{-1} down to room temperature in O_2/Ar atmosphere (similar to air, volume ratio=21: 79). The pristine LLNMO-P sample was also measured separately as a reference.

Chemical analysis. The concentration of main elements, such as Li, Ni, Mn, and P was measured by inductively coupled plasma optical emission spectroscopy (ICP-OES, iCAP 7600 Thermo Fisher Scientific). Each sample (5-10 mg) was dissolved three times in a mixture of 6 ml nitric acid and 2 ml hydrochloric acid at 80 C for 4 h in a graphite oven. Each sample was then diluted. The analyses of the elements were accomplished with four different calibration solutions and an internal standard (Sc). The range of the calibration solutions did not exceed a decade. Two or three wavelengths of each element have been used for calculation.

ON-Analyzer. The oxygen content was analyzed with the method of carrier gas hot extraction (CGHE). A commercial oxygen/nitrogen analyzer TC600 (LECO) was used. The oxygen concentration was calibrated with the certified standard KED 1025, a steel powder from ALPHA. The calibration was verified with a commercial powder (NMC 532 MTI). The calibration range was close to the concentration of the samples. The standards and the samples were weighed with a mass in the range from 1 to 3 mg (weighing accuracy ± 0.05 mg) in Sn crucibles (9-10 mm). 5 mg Graphite was added and wrapped. Combined with a Sn pellet (about 200 mg) it was put into a Ni crucible. The package was loaded in an outgassed (6300 W) high temperature graphite double crucibles. The measurements take place at 5800 W. The evolving gases CO_2 and CO were swept out by helium as an inert carrier gas and measured by infrared detectors.

XPS. X-ray photoelectron spectroscopy (XPS) measurements were conducted using a K-Alpha XP Spectrometer (Thermo Fisher Scientific, East Grinstead, U.K.). Data acquisition and processing were performed using the Thermo Avantage software, as demonstrated by K. L. Parry *et al* [1]. All samples were measured with a micro-focused, monochromatic Al Kα X-ray source (1486.6 eV) with 400 µm spot size. The K-Alpha charge compensation system was used during the measurement with electrons of 8 eV energy and low-energy argon ions to prevent localized charge accumulation. XP spectra were acquired with a concentric hemispherical analyzer at 50 eV pass energy and fitted with one or more Voigt profiles (binding energy uncertainty set to 0.2 eV) and Scofield sensitivity factors were used for quantification [2]. All spectra were calibrated to the C1s peak (C-C, C-H) at 285.0 eV and the C1s peak (carbon black) at 284.4 eV controlled by means of the well-known metallic Cu, Ag and Au photoelectron peaks, respectively.

For the evaluation of the transition metal oxidation states, a multiplet splitting fitting approach was used based on 7 peaks for the Ni2$p_{3/2}$ and 6 peaks for the Mn 3$p_{3/2}$, to describe the peak shapes with the corresponding satellite features, respectively [3-4]. Additionally, overlapping signals due to the Mn LMM Auger in the Ni 2p region and Ni LMM Auger in the Mn 2p region had to be considered.

HRTEM. High-resolution transmission electron microscopy (HRTEM) was conducted to investigate the structure at the atomic scale using a Titan 80-300 electron microscope, equipped with a CEOS image aberration corrector, a high angle annular dark field (HAADF) scanning transmission electron microscopy (STEM) detector and a Tridiem Gatan image filter (GIF). The microscope was operated at an accelerating voltage of 300 kV. TEM sample preparation was carried out by dispersing the sample powder into ethanol and then drop casting on copper grids (Quantifoil Inc.).

S1.3 Electrochemical characterization

The electrochemical performances of the pristine and acid-treated samples were tested using galvanostatic cycling in CR2032 coin-type half-cells. The coin cells were fabricated in an argon-filled glove box (MBraun, H_2O, $O_2 \leq 0.1$ ppm) with a lithium metal counter electrode (diameter: 15.6 mm , thickness: 250 μm), 200 μL $LiPF_6$ in ethylene carbonate (EC): dimethyl carbonate (DMC) 1: 1 (V/V) (LP30, BASF) as electrolyte and one Celgard 2325 membrane as a separator, respectively. A homogenous slurry of active material, conductive additive (Super P, Timcal Ltd.,) and polyvinylidene fluoride (PVDF, R6020/1001, Solvay) with a weight ratio of 80: 10: 10 was coated on an aluminum foil by doctor blade to prepare the electrode. The active mass loading of each electrode (diameter: 12 mm) was 3-4 mg cm^{-2}. The coin cells were measured at various C-rates (1/20 C or 1/100 C, 1 C=320 mA g^{-1}) between 2.0-4.8 V or even 2.0-5.0 V (*vs*. Li^+/Li) at 25 °C in a climate chamber (Binder) during the galvanostatic cycling experiments. All electrochemical measurements including electrochemical impedance spectroscopy (EIS) were carried out using a Bio-Logic VMP3 multichannel potentiostat. EIS measurements were performed using an alternating current signal of small amplitude (5 mV) over a frequency range from 1M Hz to 10 mHz. All impedance spectra were fitted with RelaxIS3 software (rdh instruments GmbH & Co. KG).

S2 Additional results and discussion

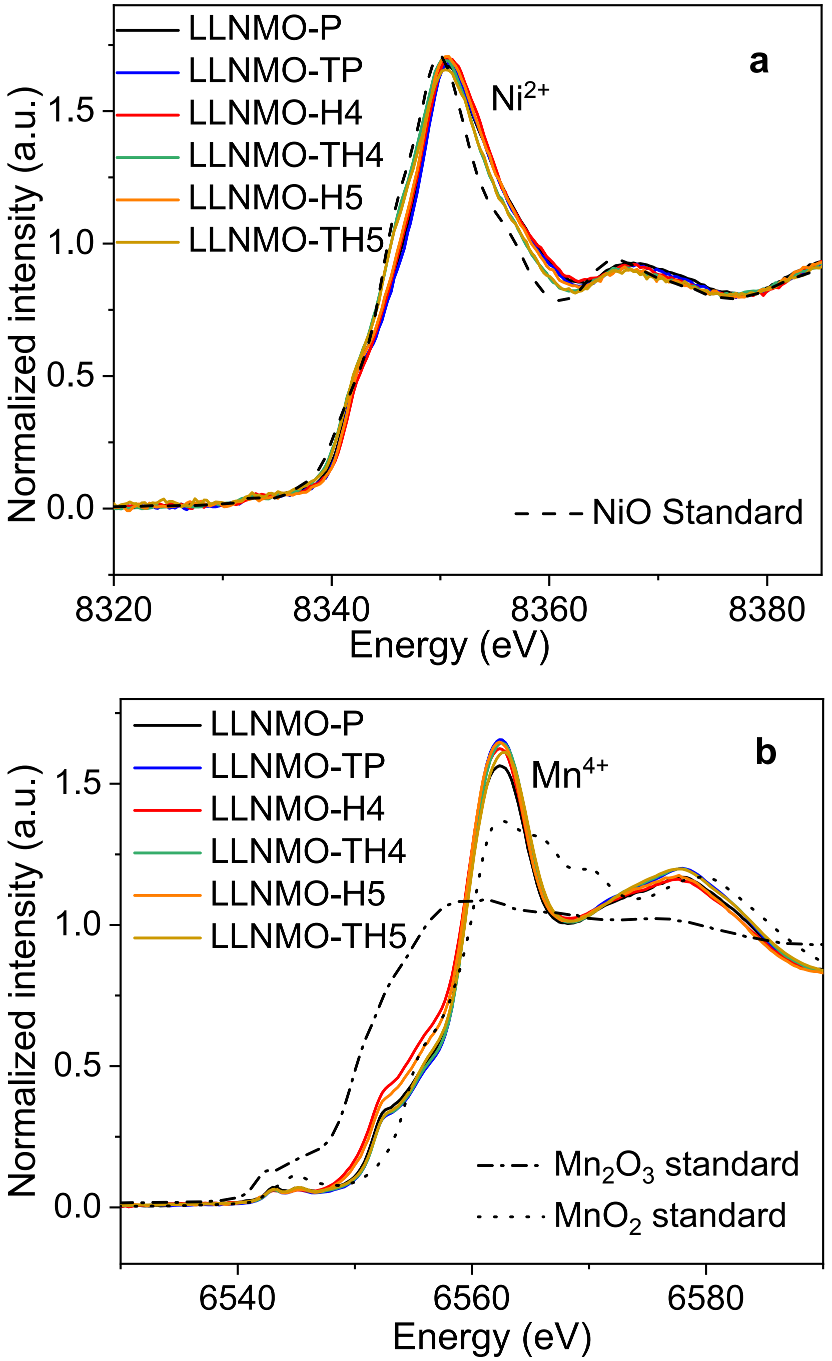

Figure S1. *Ex situ* XANES spectra at **a** Ni and **b** Mn K-edges of the LLNMO-P, LLNMO-TP, LLNMO-H4, LLNMO-TH4, LLNMO-H5 and LLNMO-TH5 samples.

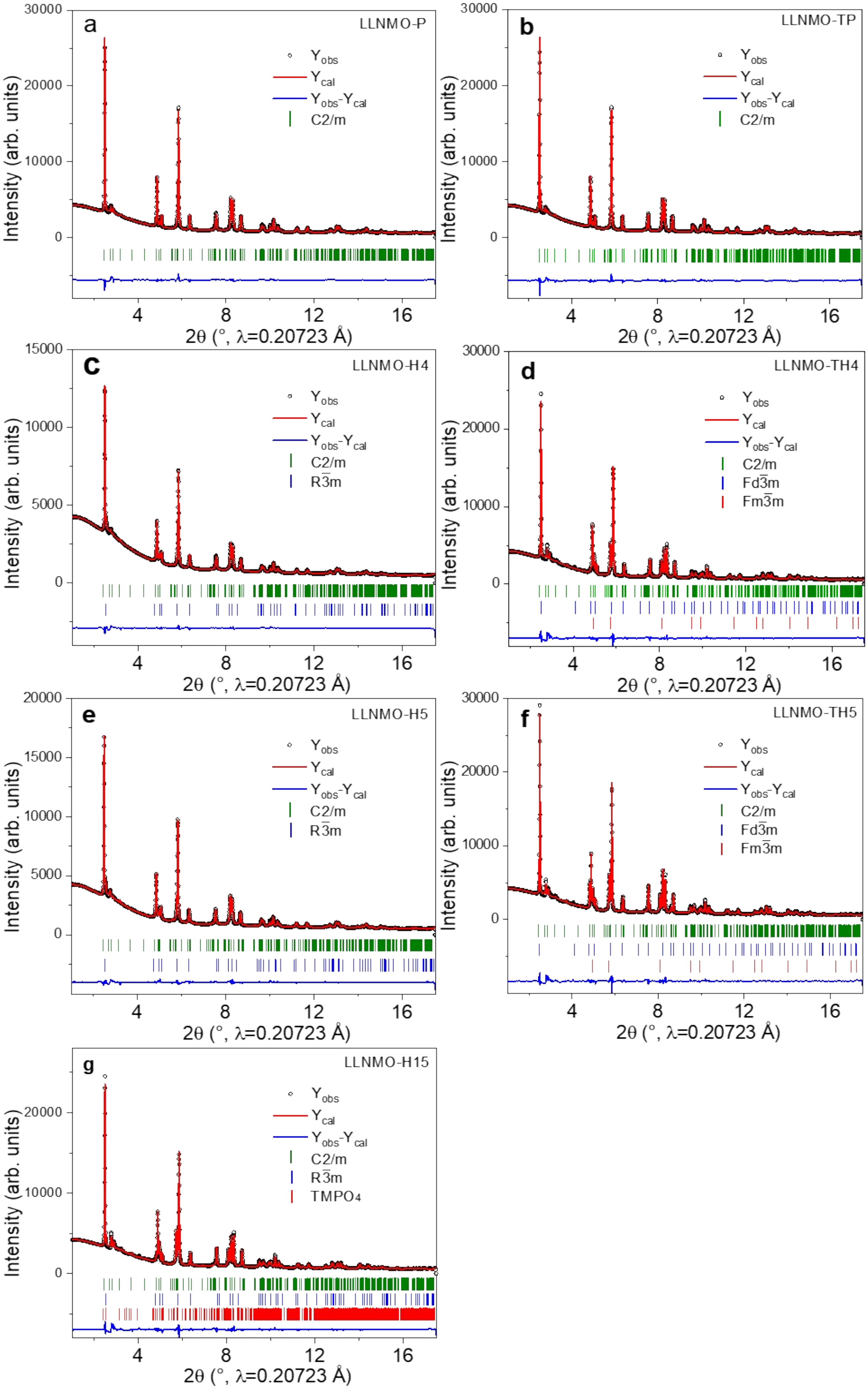
a
LLNMO-P
b
LLNMO-TP
c
LLNMO-H4
d
LLNMO-TH4
e
LLNMO-H5
f
LLNMO-TH5
g
LLNMO-H15
Y_{obs}
Y_{cal}
Y_{obs}-Y_{cal}
C2/m
R$\bar{3}$m
Fd$\bar{3}$m
Fm$\bar{3}$m
TMPO4
Intensity (arb. units)
2θ (°, λ=0.20723 Å)
0
5000
10000
15000
20000
30000
4
8
12
16

Figure S2. Rietveld refinement on synchrotron radiation diffraction (SRD) patterns of **a** LLNMO-P, **b** LLNMO-TP, **c** LLNMO-H4, **d** LLNMO-TH4, **e** LLNMO-H5, **f** LLNMO-TH5 and **g** LLNMO-H15.

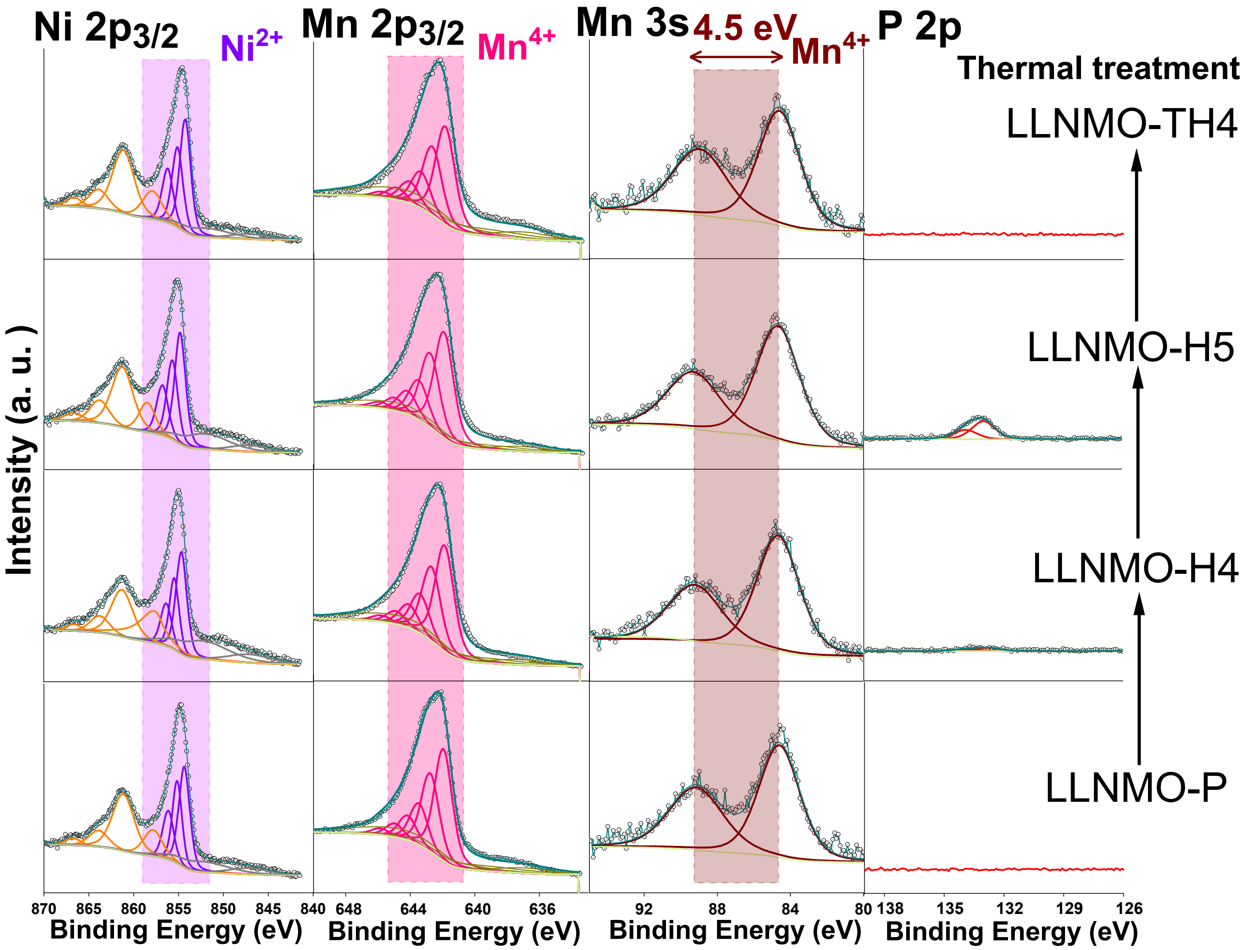

Figure S3. Ni 2p, Mn 2p, Mn 3s and P 2p spectra of LLNMO-P, LLNMO-H4, LLNMO-H5 and LLNMO-TH4.

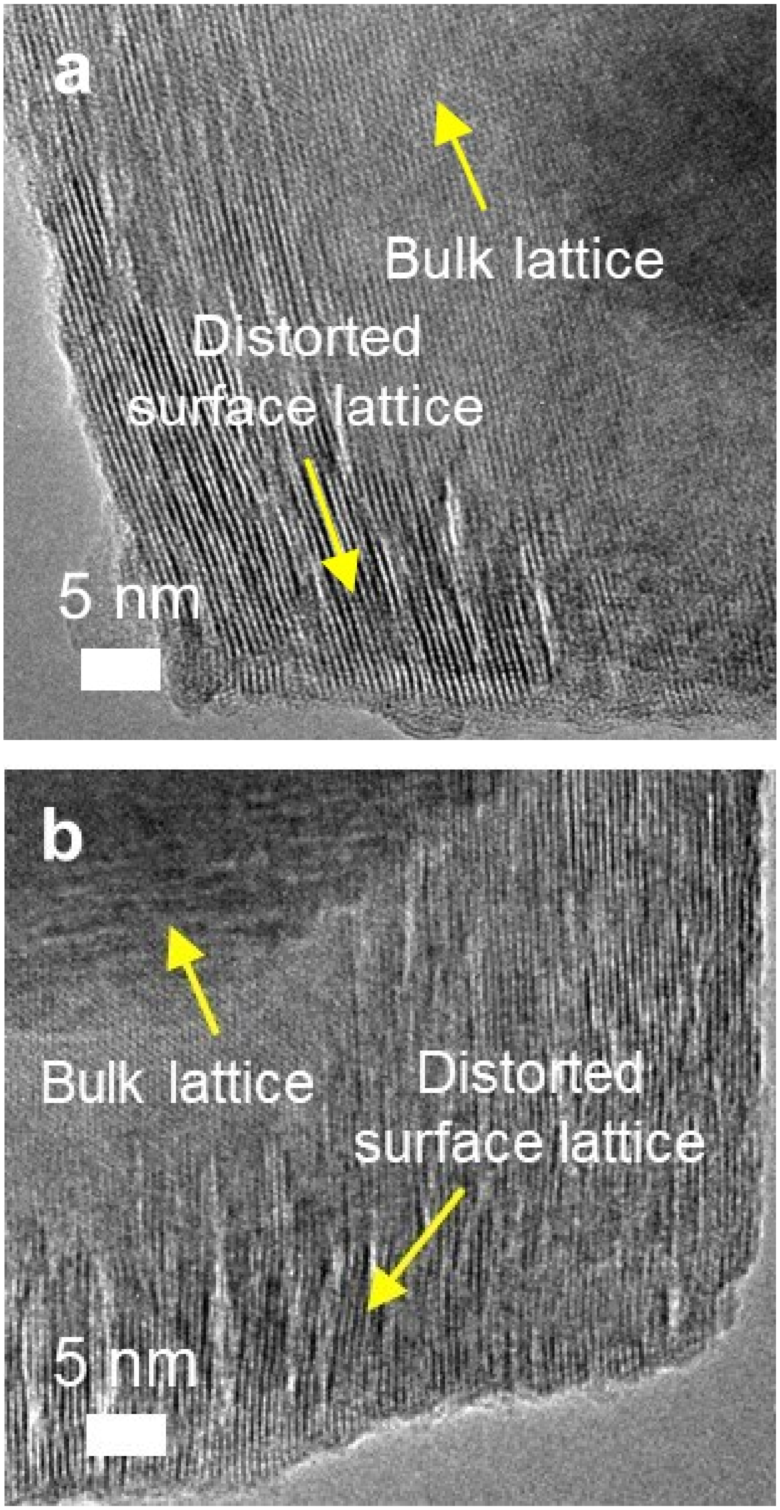

Figure S4. HRTEM images of LLNMO-H5 samples, **a** particle Nr.1 and **b** particle Nr.2, providing direct evidence for the severe lattice distortion at the near-surface region when compared with the ordered bulk lattice.

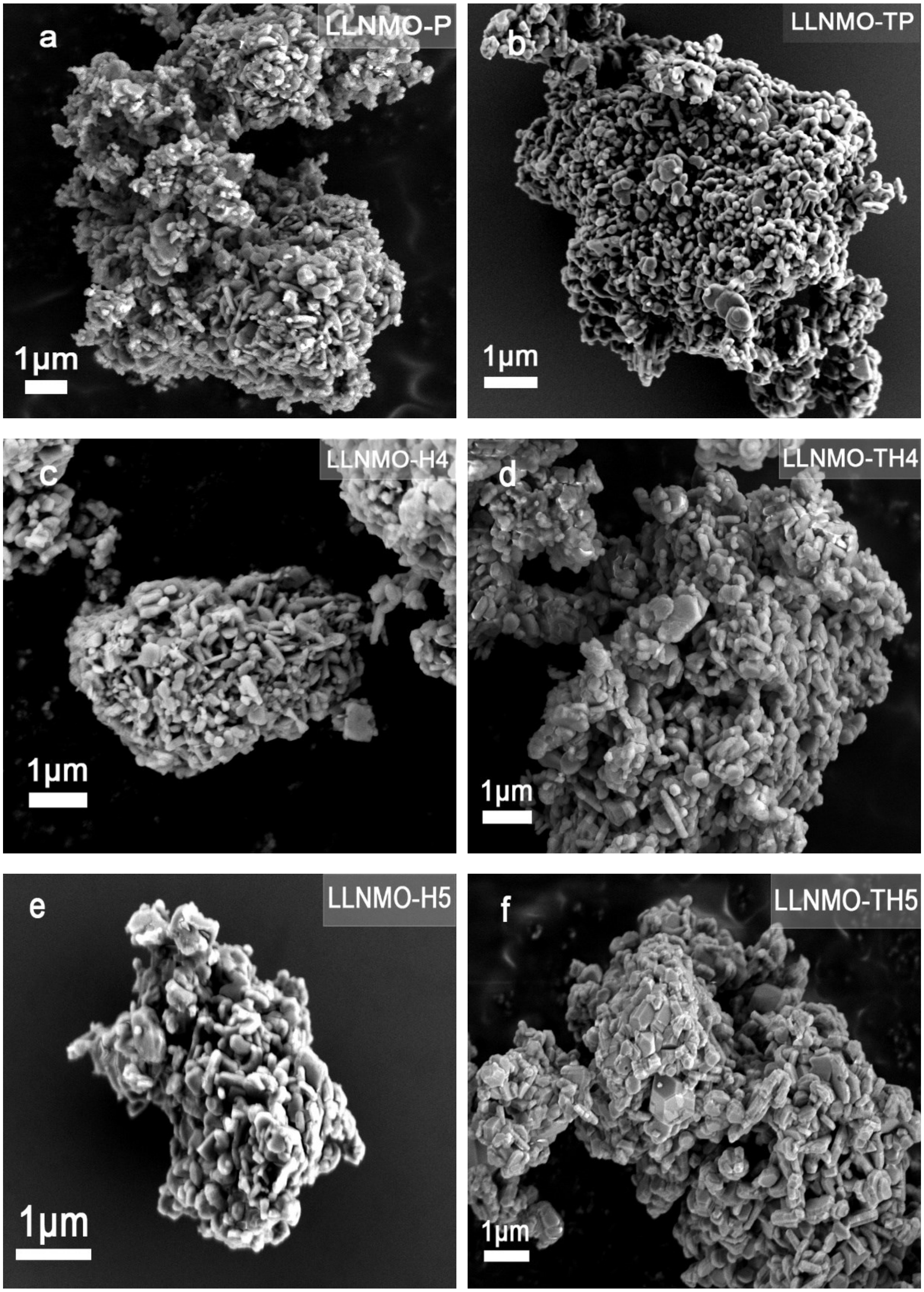

Figure S5. SEM images (overview) of the samples: **a** LLNMO-P; **b** LLNMO-TP; **c** LLNMO-H4; **d** LLNMO-TH4; **e** LLNMO-H5 and **f** LLNMO-TH5.

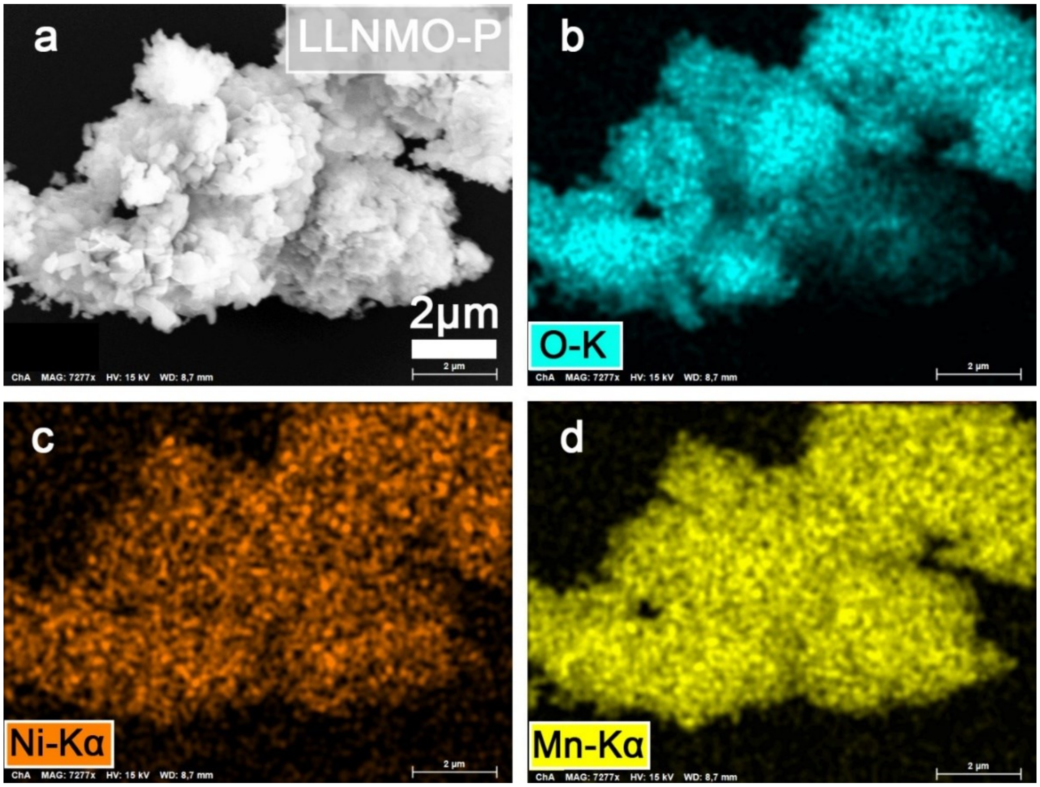

Figure S6. EDX analysis of LLNMO-P: **a** SEM micrograph of the selected area for mapping; **b-d** the elemental maps for O, Ni and Mn, respectively.

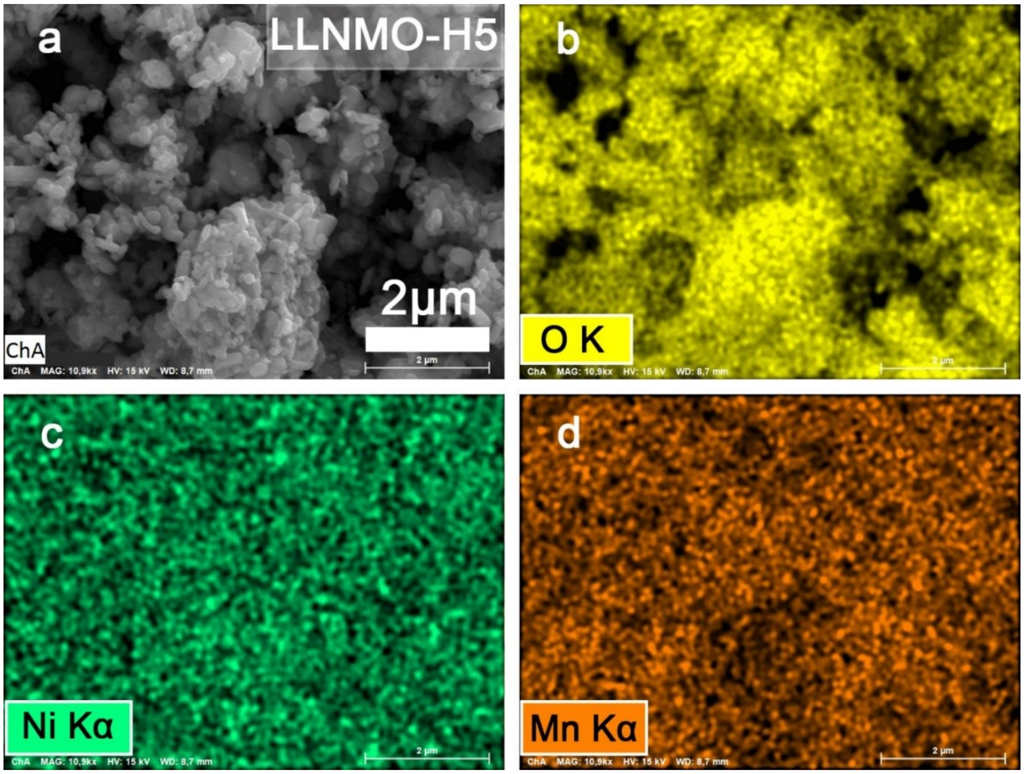

Figure S7. EDX analysis of LLNMO-H5: **a** SEM micrograph of the selected area for mapping; **b-d** the elemental maps for O, Ni and Mn, respectively.

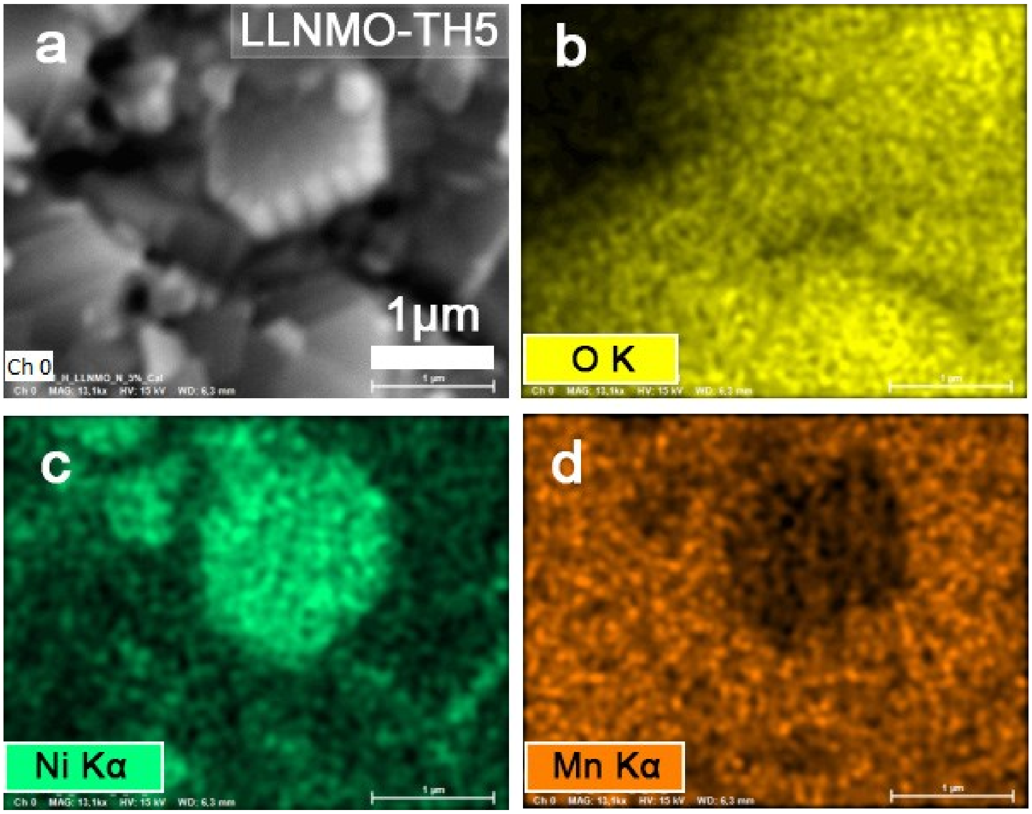

Figure S8. EDX analysis of LLNMO-TH5: **a** SEM micrograph of the selected area for mapping; **b-d** the elemental maps for O, Ni and Mn, respectively.

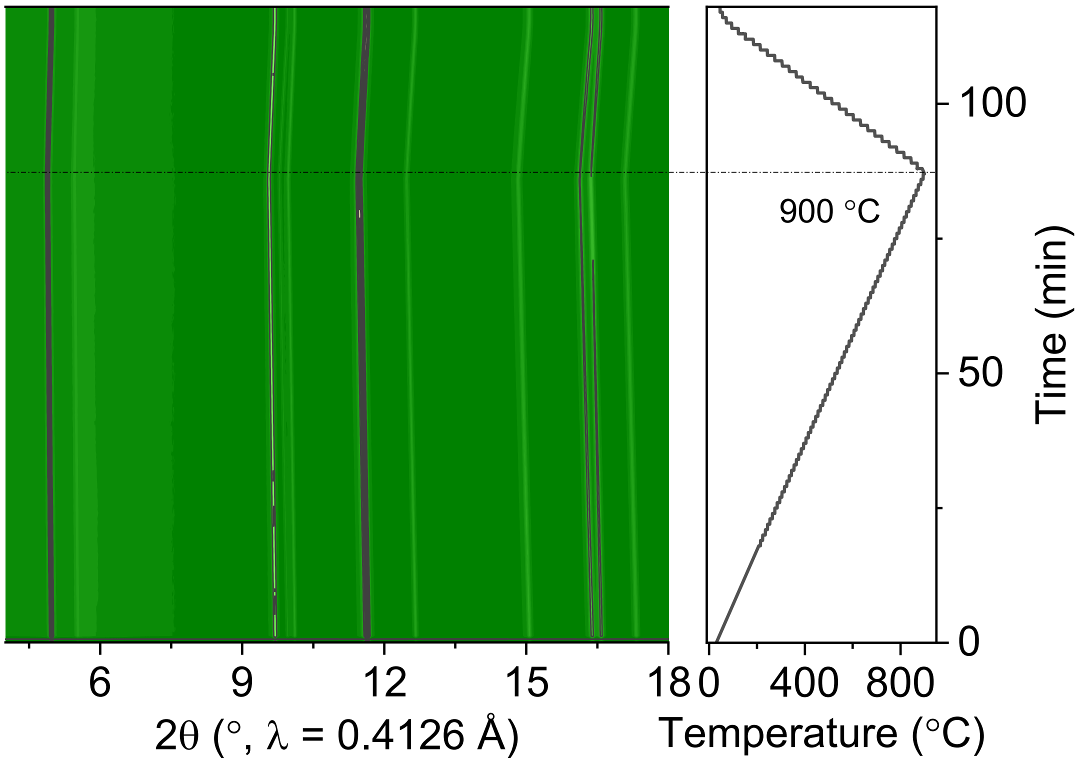

Figure S9. *In situ* HTSRD patterns of LLNMO-P. On the right side of the SRD patterns is the corresponding calcination process.

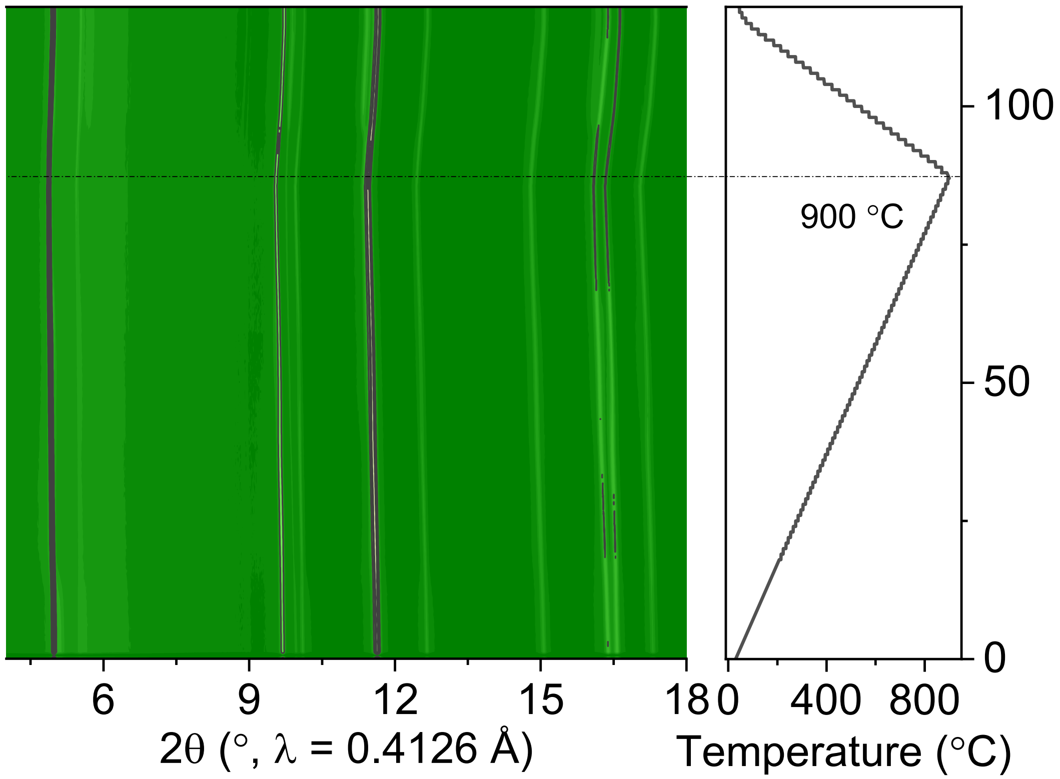

Figure S10. *In situ* HTSRD patterns of LLNMO-H4. On the right side of the SRD patterns is the corresponding calcination process.

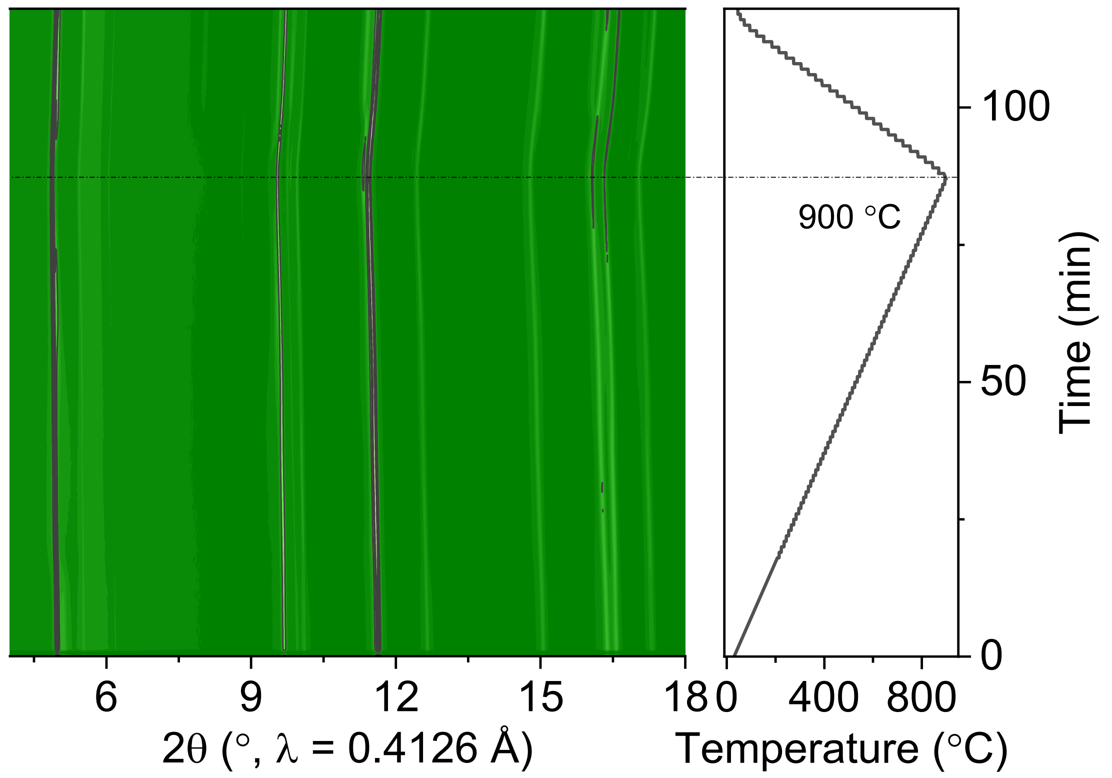

Figure S11. *In situ* HTSRD patterns of LLNMO-H5. On the right side of the SRD patterns is the corresponding calcination process.

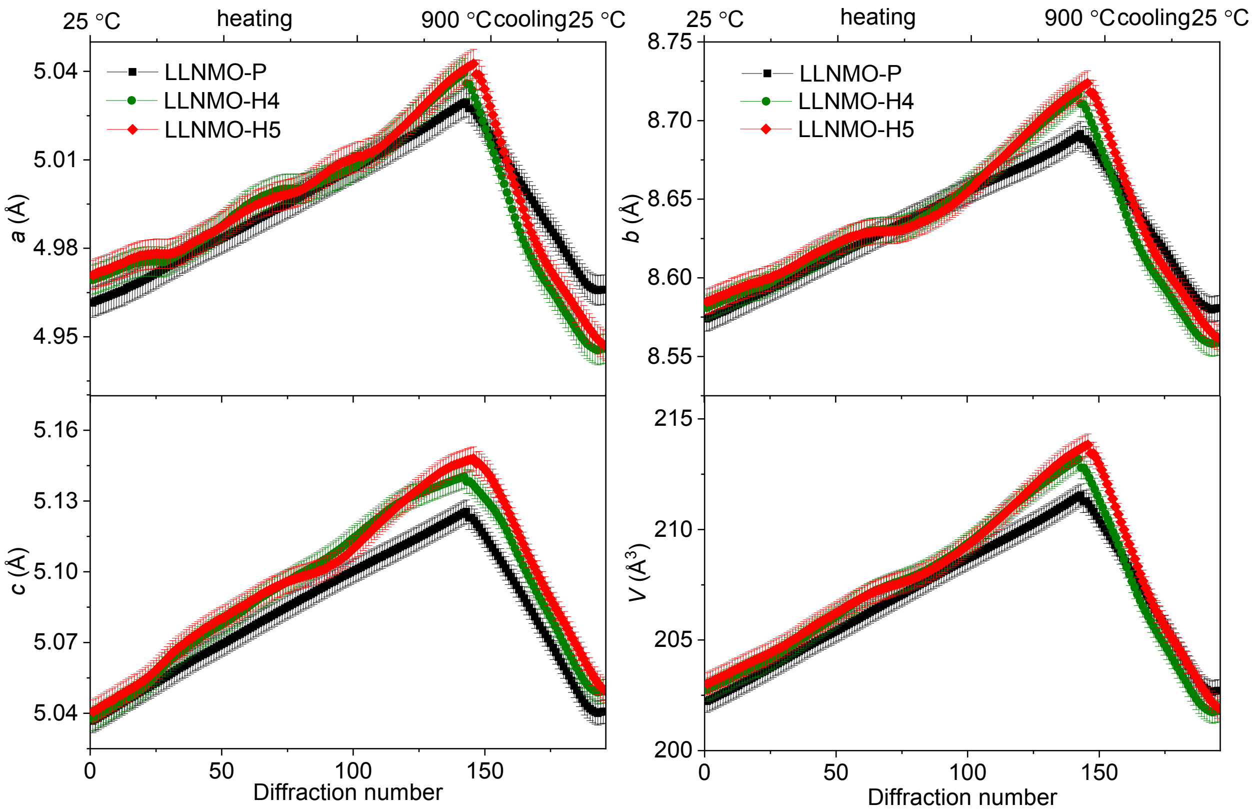

Figure S12. Lattice parameter changes (*a*, *b*, *c* and unit-cell volume *V*) of LLNMO-P, LLNMO-H4 and LLNMO-H5 during the *in situ* HTSRD measurements.

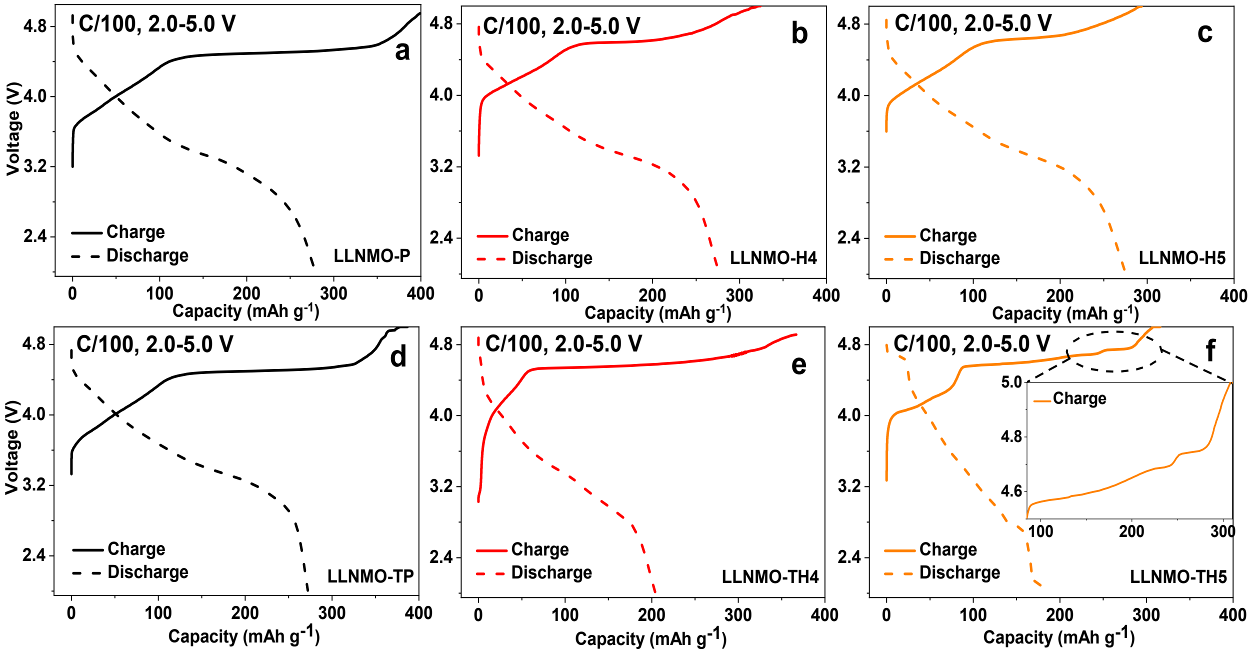

Figure S13. Initial charge-discharge voltage profiles of different LLNMO electrodes at 1.0-5.0 V at 1/100 C: **a** LLNMO-P; **b** LLNMO-H4; **c** LLNMO-H5; **d** LLNMO-TP; **e** LLNMO-TH4; **f** LLNMO-TH5.

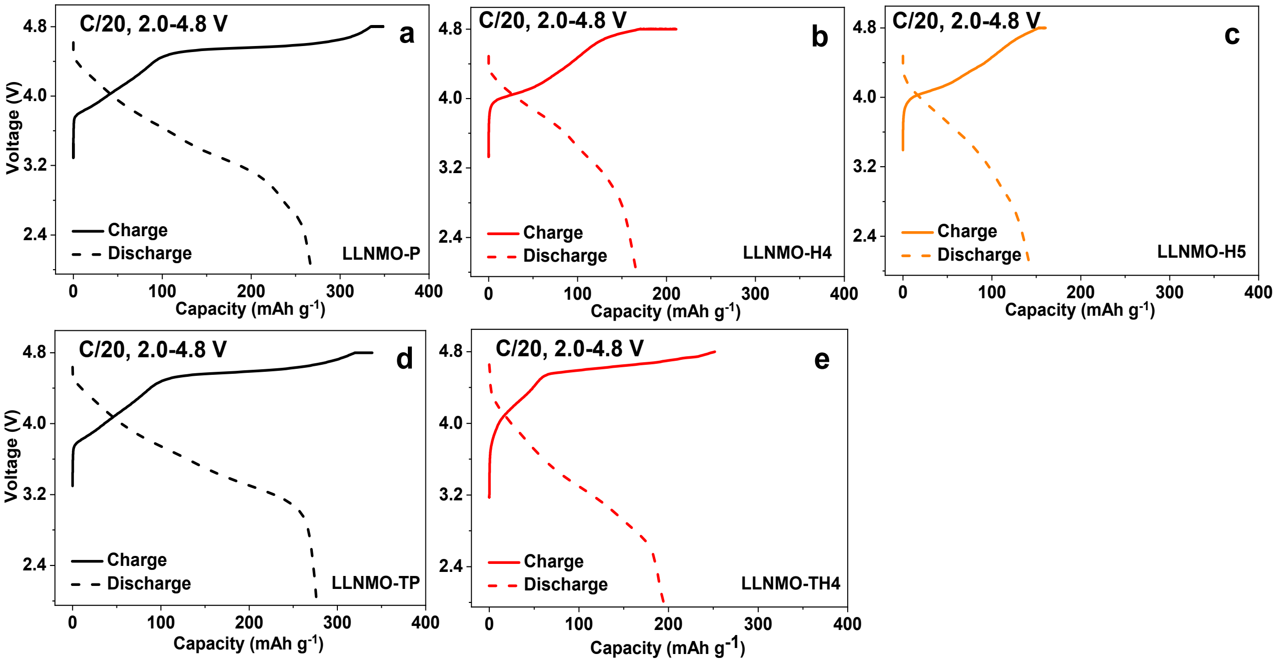

Figure S14. Initial charge-discharge voltage profiles of different LLNMO electrodes at 2.0-4.8 V at 1/20 C: **a** LLNMO-P; **b** LLNMO-H4; **c** LLNMO-H5; **d** LLNMO-TP and **e** LLNMO-TH4.

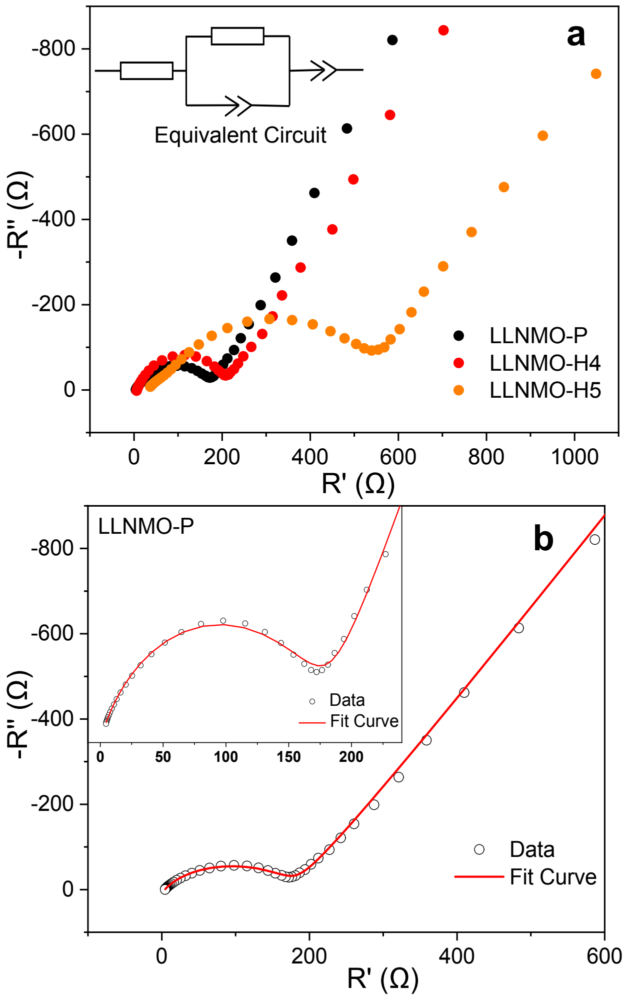
a
Equivalent Circuit
-800
-600
-400
-200
0
-R'' (Ω)
0
200
400
600
800
1000
R' (Ω)
● LLNMO-P
● LLNMO-H4
● LLNMO-H5
b
LLNMO-P
○ Data
Fit Curve
0
50
100
150
200
○ Data
Fit Curve
-800
-600
-400
-200
0
-R'' (Ω)
0
200
400
600
R' (Ω)

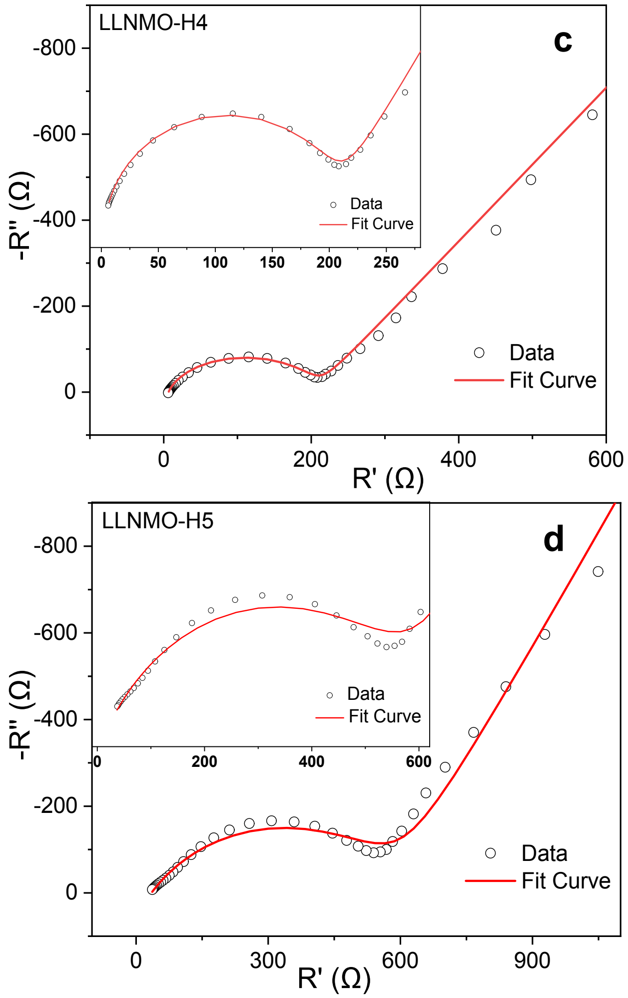

Figure S15. Impedance spectra recorded **a** and the fitting curves **b-d** of LLNMO-P, LLNMO-H4 and LLNMO-H5 electrodes before cycling. The inset in **a** is the equivalent circuit model used for fitting.

Table S1. Lattice parameters of LLNMO-P; (b) LLNMO-H4; (c) LLNMO-H5; (d) LLNMO-TP; (e) LLNMO-TH4; (f) LLNMO-TH5.

Sample	Monoclinic layered phase (*C*2/*m*)					Defective layered phase (*R-3m*)			Li-containing rock-salt phase (*Fm-3m*)		Li-containing spinel (*Fd-3m*)	
	a (Å)	*b* (Å)	*c* (Å)	beta	fraction (wt.%)	*a* (Å)	*c* (Å)	fraction (wt.%)	*a* (Å)	fraction (wt.%)	*a*(Å)	fraction (wt.%)
LLNMO-P	4.9623	8.5667	5.0353	109.362	100	/	/	/	/	/	/	/
LLNMO-H4	4.9662	8.5768	5.0341	109.326	94.09	2.8914	13.9164	5.91	/	/	/	/
LLNMO-H5	4.9680	8.5777	5.0363	109.327	91.65	2.9201	13.8984	8.35	/	/	/	/
LLNMO-TP	4.9601	8.5707	5.0346	109.323	100	/	/	/	/	/	/	/
LLNMO-TH4	4.9360	8.5506	5.0284	108.895	80.48	/	/	/	4.1484	15.08	8.1692	4.45
LLNMO-TH5	4.9360	8.5506	5.0284	108.895	72.64	/	/	/	4.1484	13.36	8.1692	14.00

Standard deviation: < 5 %.

Table S2. XPS quantification results of Li, Ni, Mn, O and P in the LLNMO-P, LLNMO-H4, LLNMO-H5 and LLNMO-TH4 samples (Atomic concentration normalized to Ni).

Samples	Relative concentration				
	Li	Ni	Mn	O	P
LLNMO-P	5.9	1.0	1.5	7.7	0.0
LLNMO-H4	2.8	1.0	2.1	8.8	0.1
LLNMO-H5	2.2	1.0	1.8	9.0	0.6
LLNMO-TH4	3.6	1.0	1.3	6.3	0.0

Standard deviation: < 10 % of atomic concentration, except for Li which is higher than 10 %.

Binding energy uncertainty: ± 0.2 eV.

Table S3. HTSRD phase fractions of LLNMO-P, LLNMO-H4 and LLNMO-H5 samples.

Sample	Temperature (°C)	Monoclinic layered phase (*C*2/*m*)					Defective layered phase (*R-3m*)			Li-containing rock-salt phase (*Fm-3m*)		Li-containing spinel (*Fd-3m*)	
		a (Å)	*b* (Å)	*c* (Å)	beta	fraction (wt.%)	*a* (Å)	*c* (Å)	fraction (wt.%)	*a* (Å)	fraction (wt.%)	*a*(Å)	fraction (wt.%)
LLNMO-H4	25	4.9710	8.5837	5.0405	109.362	97.14	2.9170	13.8996	2.86	/	/	/	/
	800	5.0379	8.7139	5.1431	109.217	92.98	/	/	/	4.1832	5.91	8.3739	1.11
	50 (after heating)	4.9459	8.5587	5.0494	109.250	83.74	/	/	/	4.1511	11.73	8.1692	4.53
LLNMO-H5	25	4.9710	8.5838	5.0405	109.295	95.05	2.9168	13.9001	4.95	/	/	/	/
	800	5.0372	8.7171	5.1475	109.210	84.03	/	/	/	4.1965	13.33	8.2976	2.64
	50 (after heating)	4.9446	8.5561	5.0468	109.2625	76.34	/	/	/	4.1461	11.86	8.2157	11.80

Standard deviation: < 5 %

Table S4. Equivalent circuit fitting parameters of LLNMO-P, LLNMO-H4 and LLNMO-H5 electrode measured before cycling.

Samples	Equivalent circuit fitting parameters					
	R_0	R_1	CPE Q1	CPE α1	CPE Q2	CPE α2
LLNMO-P	4.10	178.07	4.00×10^{-5}	0.69	0.0033	0.72
	(±0.06)	(±1.53)	$(\pm1.56\times10^{-6})$	(±0.004)	$(\pm3.17\times10^{-5})$	(±0.0028)
LLNMO-H4	6.55	197.99	2.37×10^{-5}	0.84	0.0037	0.67
	(±0.24)	(±5.37)	$(\pm2.89\times10^{-6})$	(±0.014)	$(\pm1.21\times10^{-4})$	(±0.0096)
LLNMO-H5	35.08	560.83	3.68×10^{-5}	0.60	0.0015	0.67
	(±0.90)	(±11.3)	$(\pm3.11\times10^{-6})$	(±0.009)	$(\pm3.33\times10^{-5})$	(±0.0060)

R_0, R_1: Resistance; CPE: Constant phase element; CPE α1, CPE α2: Coefficient.

Reference

1. K. L. Parry, A. G. Shard, R. D. Short, et al. ARXPS characterisation of plasma polymerised surface chemical gradients. Surf. Interface Anal., 2006, 38, 1497–1504.

2. J. H. Scofield. Hartree-Slater subshell photoionization cross-sections at 1254 and 1487 Ev. J. Electron Spectrosc. Relat. Phenom, 1976, 8, 129–137.

3. Biesinger, M. C.; Payne, B. P.; Grosvenor, A. P.; Lau, L. W. M.; Gerson, A. R.; Smart, R. S. C. Resolving Surface Chemical States in XPS Analysis of First Row Transition Metals, Oxides and Hydroxides: Cr, Mn, Fe, Co and Ni. Appl. Surf. Sci. 2011, 257 (7), 2717–2730.

4. Azmi, R.; Trouillet, V.; Strafela, M.; Ulrich, S.; Ehrenberg, H.; Bruns, M. Surface Analytical Approaches to Reliably Characterize Lithium Ion Battery Electrodes. Surf. Interface Anal. 2018, 50, 43–51.